TEPES
TURKISH JOURNAL OF
ELECTRICAL POWER
AND ENERGY SYSTEMS

TEPES, Vol. 5, Issue. 1, 41-53, 2025 **DOI:** 10.5152/tepes.2024.24028

RESEARCH ARTICLE

The Effect of Local and Interarea Oscillations of Wind Turbine Generators Based on Permanent Magnet Synchronous Generators Connected to a Power System

Cem Haydaroğlu[1], Burak Yıldırım[2], Heybet Kılıç[3], Mahmut Temel Özdemir[4]

[1]Department of Electrical and Electronics Engineering, Dicle University Faculty of Engineering, Diyarbakır, Türkiye
[2]Bingöl University, Vocational and Technology High School, Bingöl, Türkiye
[3]Department of Electric Power and Energy System, Dicle University, Diyarbakır, Türkiye
[4]Department of Electrical and Electronics Engineering, Fırat University Faculty of Engineering, Elazığ, Türkiye

Cite this article as: C. Haydaroğlu, B. Yıldırım, H. Kılıç and M. Temel Özdemir, "The effect to local and interarea oscillations of a wind turbine generators based on PMSG connected to a power system," *Turk J Electr Power Energy Syst.* 2025; 5(1), 41-53.

ABSTRACT

In this study, the effects of wind turbine generators (WTGs) based on permanent magnet synchronous generators (PMSGs) on oscillations of the power system are investigated. The analysis studies were performed for three different cases (base case, WTG based on PMSG displacement with a suitable synchronous generator, and WTG based on PMSG connection to a suitable bus without changing the synchronous generators) in Kundur's two-area power system and the IEEE 30-bus test system. It has been concluded that WTG based on PMSG can have positive and negative effects on power system oscillatory stability depending on the value of synchronous generator power replaced by WTG based on PMSG power and the location of WTG based on PMSG.

Index Terms—Eigenvalue and sensitivity analysis, local and interarea oscillation, offshore wind turbine generator (WTG), permanent magnet synchronous generators (PMSG)

I. INTRODUCTION

The fossil resources employed for energy production are being depleted at an irreversible rate, while the energy demand of modern society continues to grow daily [1,2]. Furthermore, the power plants that utilise these fuels inflict significant damage upon our planet [3-5]. The network connections of renewable energy sources represent the most effective means of addressing these issues [6,7].

Despite the challenging macroeconomic environment in 2023, the wind industry experienced its most successful year [8]. Despite the slowdown in renewable energy investments, especially due to the global health crisis triggered by COVID-19, the Red Sea crisis, and the long supply chain disruptions dating back to the Russian invasion of Ukraine, 117 GW of wind power capacity has been connected to the electricity grid [9]. Wind power is considered one of the most widely used renewable energy sources, and due to the developments in wind technologies in the last two decades, its installed capacity reached 1 TW by the end of 2023 [10]. The difficulties encountered in public and land availability for large onshore wind turbines (WTs) are pushing wind farms toward offshore power plants. In addition, stronger wind conditions at sea are continuously generating higher capacity factors, making offshore power plants more attractive. In 2023, 10.8 GW of new power plants were connected to the grid worldwide, bringing the total power of offshore wind farms in the world to 75.2 GW, and 2023 became the second year with the highest increase in installed power for offshore power plants [11-13].

Considering the recent technological developments, significant advancements have been made in wind energy generators. These advancements have led to a perceptible increase in the presence of WTs among the production technologies in recent years [14]. The fastest progression of a direct-drive WTs with Permanent Magnet Synchronous Generator (PMSG) can be attributed to bare structure, low repair cost, high reliability, and increased conversion efficiency [15,16].

Corresponding Author: Cem Haydaroğlu E-Mail: cem.haydaroglu@dicle.edu.tr

Received: September 11, 2024
Revision Requested: October 9, 2024
Last Revision Received: October 17, 2024
Accepted: October 25, 2024
Publication Date: November 18, 2024

The traditional doubly fed induction generator (DFIG) and electrically excited synchronous generators operating at partial load are less efficient than PMSG. In addition, PMSGs have fewer moving parts compared to wound rotor induction generators and electrically excited ones, are more robust, and require less maintenance [17]. The variable-speed directly driven multiple-pole PMSG wind power architecture offers reliability incentives and key maintenance as part of offshore wind power [18].

There are many publications that carry out the stability analysis studies of PMSG-based wind turbine generator (WTG) in the literature [19-23]. At the same time, publications that compare the effects of different types of WTs on power system stability are found in the literature [24-26]. There are publications that address the issue of the effects of DFIG-based WTG on local and interarea oscillatory modes with the help of mode shapes and sensitivity analysis [27,28]. In these studies, no significant literature addresses the issue of the effects of PMSG-based WTG on local and interarea oscillatory modes with the help of mode shapes and sensitivity analysis.

In [29], the potential benefits of a PMSG-based WTG additional damping controller on low-frequency oscillation (LFO) damping were explored. In this study, it is opted to use an in-domain mathematical model. The proposed method demonstrated encouraging results in terms of system damping, particularly with the inclusion of PMSG-based WTG. In [30], an attempt was made to perform a dynamic analysis of ultra-LFOs in wind-hydroelectric hybrid systems. In this study, it has been observed that WTs based on a DFIG may potentially contribute to the damping of ultra-LFO. In [31], a potential solution is put forth in the form of an optimized dynamic mode decomposition algorithm, which could help to reduce the frequency oscillations of grid-connected voltage source converters (VSCs) of synchronous generators. It is thought that this may help to reduce power oscillations. In [32], a network mode energy (NME) method is put forth as a potential means of analyzing the LFO of a power system with PMSG. It would appear that the proposed method may have the effect of reducing power oscillations. In [33], the question of power oscillation damping (POD) in WTGs based on DFIG was investigated. In this study, it was observed that power oscillations were reduced and [34] also looked at WTG to reduce POD. The study was also verified in a two-area power system. It seems that WTG may have the effect of reducing oscillations in power systems.

Main Points

- In this study, the effects of PMSG based WTG on power system oscillatory stability were investigated with the help of eigenvalue analysis.
- Analysis studies were carried out on Kundur's two area power system and IEEE 30 bus test systems and 3 different cases associated with the effects of PMSG based WTG are considered in oscillatory stability assessment of power systems by means of eigenvalue and sensitivity analysis.
- It has been concluded that because the addition of the PMSG-based WTG to the power system, the existing local and interarea modes may be lost, experienced path changes or steady depending on the location and power values of the PMSG based WTG and synchronous generators.

In this article, the effects of PMSG-based WTs on power system oscillation stability are investigated using eigenvalue and sensitivity analysis methods. The advantages of this article are listed below:

- This article offers a detailed examination of WTGs based on PMSG, which have gained recognition for their notable efficiency, reliability, and minimal maintenance needs compared to other WT types (such as DFIG).
- This article attempts to shed light on the subject of local and intra-area oscillations in power systems, which are of great importance for maintaining stability in interconnected grids. Furthermore, the eigenvalue and sensitivity analyses applied in this study offer a promising method for evaluating system stability under different conditions.
- In this paper, two widely accepted models in the field of power systems are employed: the Kundur two-area power system and the IEEE 30-bus test system.
- By examining three different scenarios (base case, replacement of synchronous generators with PMSG-based WTGs, and addition of PMSG-based WTGs), this article aims to provide a comprehensive comparison of how PMSG-based WTGs can affect system stability depending on the integration strategies, with the intention of offering insights that could be useful in future developments.
- This article responds to the growing need for renewable energy sources, particularly wind power, in modern power systems and sustainable energy solutions. It offers technical insights on how renewable technologies can be effectively integrated into power grids.
- It may be suggested that PMSG-based WTGs have the potential to improve the damping of in-field oscillations, which could be beneficial in avoiding instability in large-scale power systems. It is also possible that PMSG-based WTGs could play a role in improving grid stability in systems with a high penetration of renewable energy.

It is acknowledged that the article is not without some potential drawbacks, which could be addressed in future research. This article is based on Kundur's two-area power system and the IEEE 30-bus test system. It is possible that these models do not fully represent the complexities of real-world power grids, particularly those with highly interconnected and larger-scale systems. This article focuses on small signal stability (oscillatory stability) and does not comprehensively cover large signal stability (transient stability), which is equally important in modern power systems. Furthermore, this study assumes that the converter dynamics in PMSG-based WTGs are fast enough to ignore the effects of transients, which simplifies the analysis.

In this article, although there are some potential drawbacks, there are many advantages in power system stability, renewable energy integration, and the application of PMSG-based WTs in modern grids. For this purpose, first of all, descriptive information is given about the issue of oscillatory stability in Section II, followed by the method of eigenvalue and sensitivity analysis. In Section III, the model and equations of the PMSG-based WTG are shown. In Section IV of the paper, the effects of the PMSG-based WTG on the power system oscillatory stability are analyzed. Finally, results are presented in Section V.

II. EIGENVALUE AND SENSİTİVİTY ANALYSİS

The oscillatory stability issue is investigated in rotor angle stability [35]. Angle stability, or rotor angle stability, can be defined as the capability of interconnected synchronous machines to remain in synchronization. Angle stability is divided into two main subcategories: small signal angle stability and transient angle stability [35,36]. Small signal (also called small disturbance or oscillation) rotor angle stability is associated with the ability of generators to maintain their synchronization after small disturbances [36]. There are two types of electromechanical oscillations [36,38].

Local mode oscillations: They are oscillations associated with the oscillations of units in a production station relative to the rest of the power system.

Interarea mode oscillations: They are oscillations associated with the oscillations of many machines in one part of the power system against machines in other areas or other parts of the power system.

The ordinary differential algebraic equations represented by (1) can be used to express the small signal stability of the power system. The small disturbance stability of the power system [39,40]

$$\dot{x} = f(x,u) \quad y = g(x,u) \tag{1}$$

In (1), *x*, *y,* and *u* indicate the vector of state variables, output variable, and input variables, whereas *f* and *g* are functions of the state and the output variables.

The modal analysis, which defines the dynamic behavior of the system when it is subjected to a minor disturbance, is derived by linearizing Eq. (1) around a given operating point. A set of state-space equations shown in (2) indicates linearized equations.

$$\Delta\dot{x} = A\Delta x + B\Delta u \quad \Delta y = C\Delta x + D\Delta u \tag{2}$$

In (2), *A*, *B*, and *C* are used to show state, input, and output matrices. The *D* matrix defines the connection between input and output variables. Important information on the oscillation conditions and the system dynamic response is derived from the eigenvalues of the state matrix *A*. The stability of the system is determined by looking at the eigenvalues of the system.

The time-dependent characteristic of the mode associated with a λ_i eigenvalue is given by $e^{-\lambda_i t}$. For a complex pair of eigenvalues:

$$\begin{aligned} \lambda_i &= \sigma + j\omega \\ f &= \omega / 2\pi \\ \zeta &= -\sigma / \sqrt{\sigma^2 + \omega^2} \end{aligned} \tag{3}$$

Where *f* is the frequency in Hz, ζ shows the damping rate.

$$p_{ki} = \phi_{ki}\psi_{ki} \tag{4}$$

Where φ_{ki} and ½$_{ki}$ show the right and left eigenvector elements, respectively. The participation factor (P_{ki}), which is a combination of right and left eigenvectors, gives a measure of the relationship between state variables and modes [41].

$$p_{ki} = \partial\lambda_i / \partial a_{kk} \tag{5}$$

III. PMSG-BASED WTG MODEL

Because the rotor and stator flux dynamics are fast with reference to grid dynamics and the converter controls mainly decouple the generator from the grid, steady-state electrical equations of the PMSG are supposed. The PMSG-based WTG Model is given in Fig. 1. As a consequence of these suppositions,

$$v_{ds} = -r_S i_{ds} + \omega_m x_q i_{qs}, \qquad v_{qs} = -r_S i_{qs} - \omega_m \left(x_d i_{ds} - \psi_p \right) \tag{6}$$

in (6), the rotor circuit is shown by permanent field flux ½*p*. The (7) indicates active and reactive powers of the generator.

$$P_s = v_{ds} i_{ds} + v_{qs} i_{qs} \qquad Q_s = v_{qs} i_{ds} + v_{ds} i_{qs} \tag{7}$$

The active and reactive powers are injected into the grid based solely on the grid side currents of the converter:

$$P_c = v_{dc} i_{dc} + v_{qs} i_{qs} \qquad Q_c = v_{qc} i_{dc} + v_{dc} i_{qc} \tag{8}$$

In (8), the grid voltage magnitude and phase are used to represent the converter voltages, as follows:

$$v_{dc} = V\sin(-\theta) \qquad v_{qc} = V\sin\theta \tag{9}$$

Assessing a power factor equal to 1 and a lossless converter, the output power of the generator becomes the following:

$$P_s = P_c \qquad Q_s = 0 \tag{10}$$

Additionally, the converter direct current i_{dc}, which allows rewriting the second equation of (8), controls the reactive power injected into the grid. The second part of (8) is written as the following:

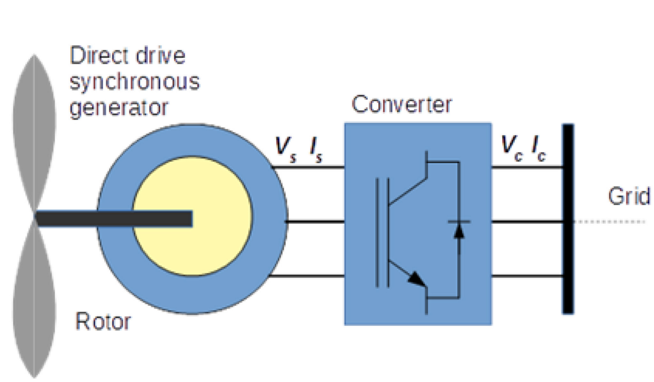

Fig. 1. Permanent magnet synchronous generator (PMSG)-based wind turbine generator (WTG) model.

$$Q_c = \frac{1}{\cos\theta} V i_{dc} + \tan\theta P_s \tag{11}$$

Assessing converter controls can filter shaft dynamics; a single shaft models generator motion equation. Due to a similar reason, tower shadow effect is not taken into account in the PMSG model. Therefore:

$$\dot{\omega}_m = \left(T_m - T_e\right) / 2H_m \qquad T_e = \psi_{ds} i_{qs} - \psi_{qs} i_{ds} \tag{12}$$

The (12) indicates the connection between generator currents and stator fluxes.

$$\psi_{ds} = -x_d i_{ds} + \psi_p \qquad \psi_{qs} = -x_q i_{qs} \tag{13}$$

The following equations are used to model mechanical torque and power:

$$T_m = P_\omega / \omega_m \tag{14}$$

The P_ω mechanical power indicates the power extracted from the wind. The second of these is a function the rotor speed ω_m, the pitch angle ϑ_p and the wind speed v_ω. P_ω can be computed approximately as follows.

$$P_w = \frac{\rho}{2} c_p\left(\lambda, \theta_p\right) A_r v_\omega^3 \tag{15}$$

The curve $c_p(\lambda,\vartheta_p)$ approximates as follows:

$$c_p = 0.22\left(\frac{116}{\lambda_i} - 0.4\theta_p - 5\right) e^{-\frac{12.5}{\lambda_i}}, \qquad \frac{1}{\lambda_i} = \frac{1}{\lambda + 0.08\theta_p} - \frac{0.035}{\theta_p^3 + 1} \tag{16}$$

Since the converter dynamics are fast in accordance with the electromechanical transients, they are largely simplified. Therefore, the converter is considered an ideal current source, where i_{dc}, i_{qs}, and i_{ds} are state variables and are used for voltage control, the rotor speed control, and the reactive power control, respectively. Equation 17 indicates the differential equations of the converter currents.

$$\begin{aligned} \dot{i}_{qs} &= \left(i_{qsref} - i_{qs}\right) / T_{\epsilon p}, \\ \dot{i}_{ds} &= \left(i_{dsref} - i_{ds}\right) / T_{\epsilon q}, \\ \dot{i}_{dc} &= (K_V\left(V_{ref} - V\right) - i_{dc}) / T_V \end{aligned} \tag{17}$$

$$i_{qsref} = P_\omega^*\left(\omega_m\right) / \omega_m\left(\psi_p - x_d i_{ds}\right), \qquad i_{dsref} = \frac{\psi_p}{x_d} - \sqrt{\frac{\psi_p^{\,2}}{x_d^{\,2}} - \frac{Q_{ref}}{\omega_m x_d}} \tag{18}$$

In (18), $P_\omega^*\left(\omega_m\right)$ indicates the power-speed characteristic which is calculated using the current rotor speed value and which highly optimizes the wind energy capture. It is supposed that $P_\omega^* = 1\,p.u.$ if $\omega_m >$ 1 p.u. and that $P_\omega^* = 0\,p.u.$ if $\omega_m < 0.5$ p.u. Therefore, the rotor speed control merely has an effect for sub-synchronous speeds. The anti-windup limiters are applied to both the voltage and speed controls in order to avoid converter over-currents. Current limits are indicated in (19).

$$i_{qsmax} = -P_{min}, i_{qsmin} = -P_{max} \quad , i_{dsmax} = i_{dcmax} = -Q_{min}, i_{dsmin} = i_{dcmin} = -Q_{max} \tag{19}$$

The pitch angle control is described by the differential equation (20) [42]:

$$\dot{\theta}_p = \left(K_p \phi\left(\omega_m - \omega_{ref}\right) - \theta_p\right) / T_p \tag{20}$$

IV. NUMERIC RESULTS

The effects on the power system of PMSG-based WTG were investigated on the Kundur's two-area power system [41] shown in Fig. 2 and on the IEEE 30-bus test system [43] shown in Fig. 3. In order to show the effects of the PMSG-based WTG on the power system oscillatory stability, eigenvalue and sensitivity analyses were performed in both Kundur's two-area power system and the IEEE 30-bus test system for the following three cases. The power value of Generator

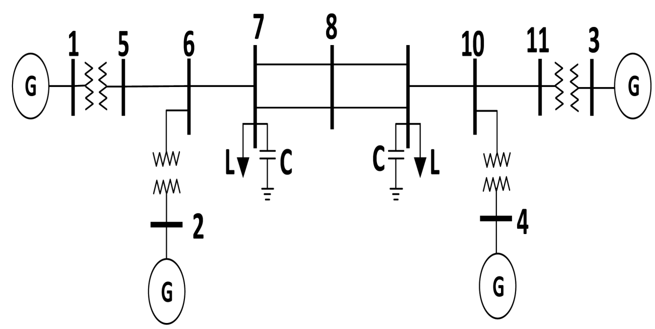

Fig. 2. Kundur's two-area power system [41].

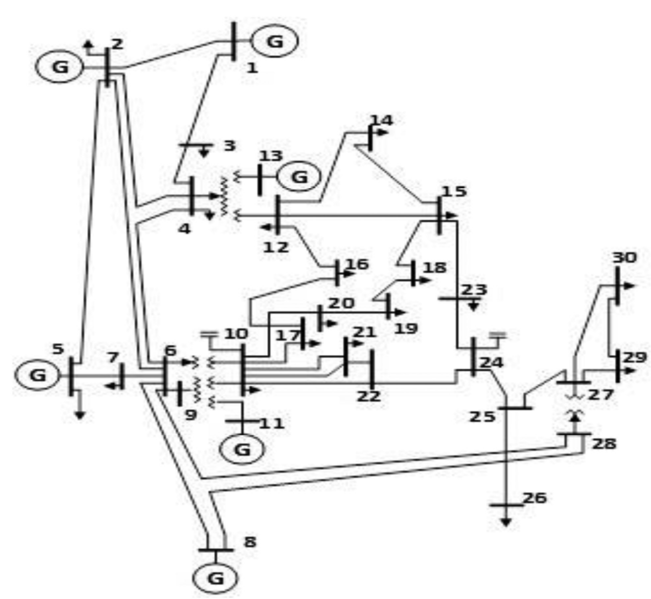

Fig. 3. IEEE 30-bus test system [33].

2 in the IEEE 30-bus power system used in the literature has been increased by 100 MW to better demonstrate the effects of PMSG-based WTG.

Case 1: Base case for both Kundur's two-area power system and the IEEE 30-bus test system.

Case 2: In Kundur's two-area power system, the synchronous generator at bus 1 is replaced by the PMSG-based WTG with the same power. In the IEEE 30-bus test system, the synchronous generator at bus 2 is replaced by the PMSG-based WTG with the same power.

Case 3: A PMSG-based WTG with a power of half of Generator 1 has been added to bus 5 for the base case system in Kundur's two-area power system. In the IEEE 30-bus test system, a PMSG-based WTG with a power of half of Generator 2 is added to bus 2 for the base case system.

A. Analysis Results for Kundur's Two-Area Power System

In Fig. 4 and Table I, the results of eigenvalue analysis for Kundur's two-area power system case 1 are given. In addition, the results of the sensitivity analysis performed for Kundur's two-area power system case 1 are given in Table I. ΔSyn and ωSyn show the rotor angles and rotor speeds of generators. Finally, the mode shapes of case 1 are shown in Fig. 5.

When Fig. 4 is examined, the power system is stable because all of the eigenvalues of the power system are on the left side of the imaginary axis. In case 1, sensitivity analysis results showed that there are two local and one interarea modes in this power system.

Local and interarea oscillation modes are determined by calculating the participation rates of rotor speed state variables of synchronous generators to modes. By looking at the contributions of synchronous generators in the areas, it is decided which areas where the local modes belong to. In interarea mode, this mode is determined as the mode to which all generators contribute. It was found that the oscillation frequencies of the modes of this system are 1–2 Hz for local oscillations and less than 1 Hz for interarea mod in accordance with the literature.

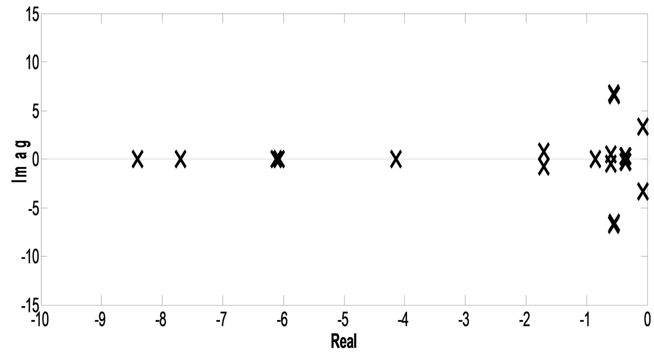

Fig. 4. Eigenvalues for Kundur's two-area power system case 1.

Mode shapes for case 1 (eigenvector components associated with the rotor speeds of synchronous generators) are shown in Fig. 5. Mode shapes provide great convenience in determining and examining local and interarea modes. As can be seen from the mode figures, the mode with a 0.53 Hz frequency is an interarea mode, and Gen1 and Gen2 generators of area 1 shows mutual oscillations with the Gen3 and Gen4 generators of area 2. The same event can be seen for the local mode area 1 with a 1.049 Hz frequency, where Gen1 and Gen2 in the same area oscillate against each other. In the local mode with 1.08 Hz frequency, Gen3 and Gen4 in area 2 show oscillations against each other. In local modes, the oscillation dimensions of the generators in the other area are very small.

In Fig. 6 and Table II, the results of eigenvalue analysis for Kundur's two-area power system case 2 are given. In addition, the results of the sensitivity analysis performed for Kundur's two-area power system case 2 are given in Table II. Finally, the mode shapes of case 2 are shown in Fig. 7.

When Fig. 6 is examined, the power system is stable because all of the eigenvalues of the power system are on the left side of the

TABLE I.
EIGENVALUES AND PARTICIPATION FACTORS FOR KUNDUR'S TWO-AREA POWER SYSTEM CASE 1

EM mod	*Eigenvalue*	*Freq*	*Damping*	*Participation Factor*				*Mod*
				Gen1 (ΔSyn1 ωSyn1)	*Gen2 (ΔSyn2 ωSyn2)*	*Gen3 (ΔSyn3 ωSyn3)*	*Gen4 (ΔSyn4 ωSyn4)*	
1	−0.554 + 6.788	1.080	0.081	0.0048	0.0078	0.2166	0.2942	Local mod-
2	−0.554 − 6.788	1.080	0.081	0.0048	0.0078	0.2166	0.2942	Local mod-
3	−0.544 + 6.597	1.049	0.082	0.2236	0.2862	0.0100	0.0039	Local mod-
4	−0.544 − 60544	1.049	0.082	0.2236	0.2862	0.0100	0.0039	Local mod-
5	−0.067 + 3.34	0.531	0.02	0.0777	0.0381	0.2274	0.1708	Interarea mod
6	−0.067 − 3.34	0.531	0.02	0.0777	0.0381	0.2274	0.1708	Interarea mod

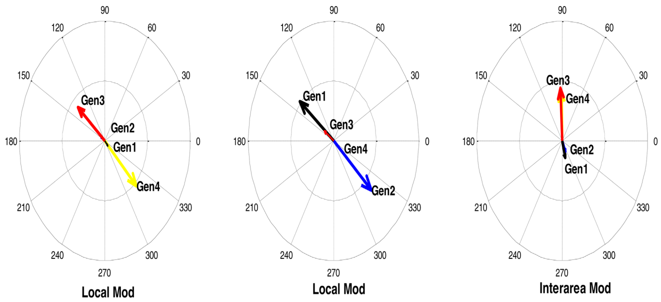

Fig. 5. Mode shapes of rotor angle modes for Kundur's two-area power system case 1.

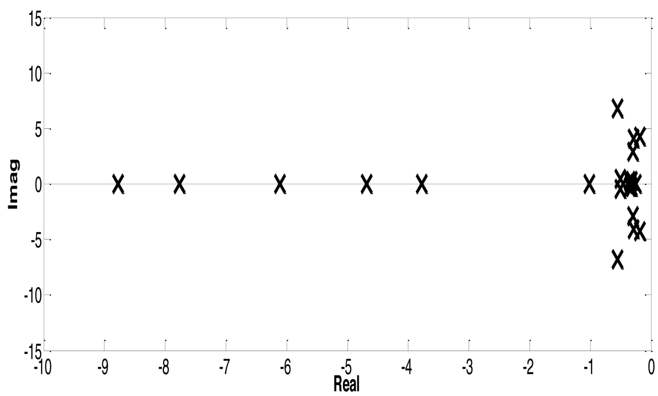

Fig. 6. Eigenvalues for Kundur's two-area power system case 2.

imaginary axis. In case 2, sensitivity analysis results showed that there is one local and two interarea modes in this power system.

For case 2, the synchronous generator in bus 1 is replaced by a PMSG-based WTG with the same power. When Table II is examined, there is no effect of the addition of the PMSG-based WTG on the local mode between Gen3 and Gen4 according to case 1. This result shows that WTG does not affect the local mode in distant areas [44]. Due to the separation of the PMSG-based WTG from the power system by power electronics converters, the PMSG-based WTG does not react to oscillations [45] and eliminates the local mode 2 in case 1. This local mode has been replaced a new interarea mode.

When the effects of PMSG-based WTG on interarea mode for case 2 are examined, it provides a damping effect to this mode of the power system and has improved the power system in terms of oscillatory stability. By adding WTs to the power system, existing synchronous generators contribute less to meeting power demand. However, because the system topology remains unchanged, the ratio of synchronous generators to the impedance of the network will be reduced. Therefore, in many cases, the joint coupling will be strengthened. The strengthening of this joint coupling allows damping oscillations between synchronous generators [43]. This explains the result of the damping improvement for interarea oscillations in case 2.

Mode shapes for case 2 are shown in Fig. 7. As seen in the mode figures, the PMSG-based WTG has no effect on either local and interarea modes. The modes with 0.675 Hz and 0.468 Hz frequency are interarea modes, and Gen2 generator of area 1 shows mutual oscillations with the Gen3 and Gen4 generators of area 2. In the local mod with a 1.078 Hz frequency, Gen3 and Gen4 in area 2 show oscillations against each other.

In Fig. 8 and Table III, the results of eigenvalue analysis for Kundur's two-area power system case 3 are given. In addition, the results of the sensitivity analysis performed for Kundur's two-area power system case 3 are given in Table III. Finally, the mode shapes of case 2 are shown in Fig. 9.

When Fig. 8 is examined, the power system is stable because all of the eigenvalues of the power system are on the left side of the imaginary axis. In case 3, sensitivity analysis results showed that there are 2 local modes and 1 interarea mode oscillations in this power system.

For case 3, a PMSG-based WTG with a power of half of Gen1 has been added to bus 5 for the base case system in Kundur's two-area power system. When Table III is examined, there is no effect on the local mode

TABLE II.
EIGENVALUES AND PARTICIPATION FACTORS FOR KUNDUR'S TWO-AREA POWER SYSTEM CASE 2

EM mod	Eigenvalue	Freq	Damping	Participation Factor Gen1 (*ΔSyn1 ωSyn1*)	Gen2 (*ΔSyn2 ωSyn2*)	Gen3 (*ΔSyn3 ωSyn3*)	Gen4 (*ΔSyn4 ωSyn4*)	Mod
1	−0.555 + 6.779	1.078	0.0815	0	0.0018	0.2272	0.297	Local mod-
2	−0.555 − 6.779	1.078	0.0815	0	0.0018	0.2272	0.297	Local mod-
3	−0.181 + 4.242	0.675	0.0426	0	0.45	0.0264	0.0424	Interarea mod
4	−0.181 − 4.242	0.675	0.0426	0	0.45	0.0264	0.0424	Interarea mod
5	−0.302 + 2.944	0.468	0.1020	0	0.0895	0.2454	0.1385	Interarea mod
6	−0.302 + 2.944	0.468	0.1020	0	0.0895	0.2454	0.1385	Interarea mod

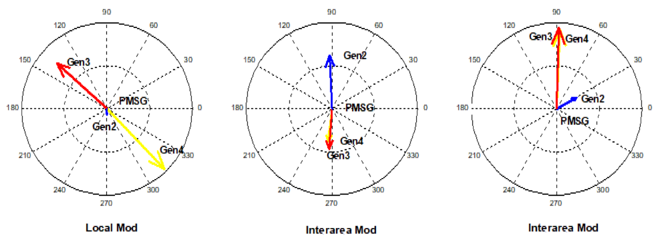

Fig. 7. Mode shapes of rotor angle modes for Kundur's two-area power system case 2.

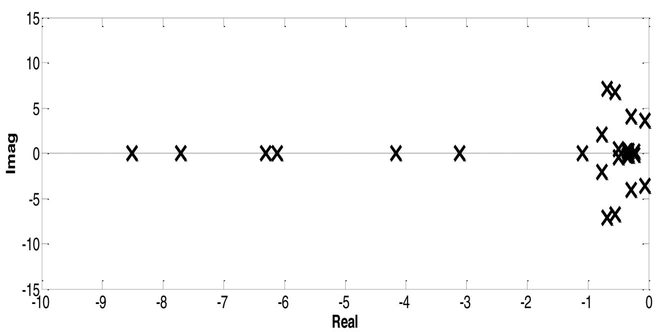

Fig. 8. Eigenvalues for Kundur's two-area powersystem case.

between Gen3 and Gen4, while has positive effect on the local mode between Gen1 and Gen2 due to the addition of the PMSG-based WTG, according to case 1. Since the WTG does not affect the local mode in distant areas, there is no effect on the local mode between Gen3 and Gen4. By adding the PMSG-based WTG to the power system, existing synchronous generators contribute less to meeting power demand. However, because the system topology remains unchanged, the ratio of synchronous generators to the impedance of the network will be reduced. Therefore, in many cases, the joint coupling will be strengthened. The strengthening of this joint coupling allows damping oscillations between synchronous generators [45]. As a result, the damping ratio of the local mode between Gen1 and Gen2 will increase.

The addition of PMSG-based WTG has a negative effect on the interarea mode. The undamped oscillation risk in power systems can be caused by large synchronous generator concentrations and comparatively weak links [41]. If a generator usually matches poorly with the remainder of the power system and is larger than the power system size, the damping rate in this area will decrease. Gen1 and Gen2's contribution to generation by adding PMSG-based WTG to area 1 will decrease. Area 2 generators will become much larger than area 1 generators, and the two areas will match poorly. The contribution of area 1 to the damping torque will be reduced, and as a result, the interarea damping will decrease.

Mode shapes for case 3 are shown in Fig. 9. As seen in the mode figures, the PMSG-based WTG has no effect on either local and interarea modes. As can be seen from the mode figures, the mode with 0.576 Hz frequency is an interarea mode, and Gen1 and Gen2 generators of area 1 shows mutual oscillations with the Gen3 and Gen4 generators of area 2. In the local mod with 1.079 Hz frequency, Gen3 and Gen4 in area 2 show oscillations against each other. Likewise, Gen1 and Gen2 in area 1 show oscillations against each other in the local mod with 1.113 Hz frequency.

B. Analysis Results for IEEE 30-Bus Test System

In Fig. 10 and Table IV, the results of eigenvalue analysis for IEEE 30-bus test system case 1 are given. In addition, the results of the sensitivity analysis performed for IEEE 30-bus test system case 1 are given in Table IV. Finally, the mode shapes of case 1 are shown in Fig. 11.

When Fig. 10 is examined, the power system is stable because all of the eigenvalues of the power system are on the left side of the imaginary axis. In case 1, sensitivity analysis results showed that there are four local modes and one interarea mode oscillations in this power system.

Mode shapes for case 1 are shown in Fig. 11. As can be seen from the mode figures and Table IV, the mode with 0.172 Hz frequency is an interarea mode, and all generators contribute to this mode. Gen 5-6, Gen 2-5-6, Gen 2-3-4, and Gen 3-4 contribute to the local modes with 1.798, 1.646, 1.4, and 1.247 Hz frequency, respectively.

TABLE III.
EIGENVALUES AND PARTICIPATION FACTORS FOR KUNDUR'S TWO-AREA POWER SYSTEM CASE 3

				Participation Factor					
EM mod	Eigenvalue	Freq	Damping	DDSG $\omega ddsg$	Gen1 ($\Delta Syn1\ \omega Syn1$)	Gen2 ($\Delta Syn2\ \omega Syn2$)	Gen3 ($\Delta Syn3\ \omega Syn3$)	Gen4 ($\Delta Syn4\ \omega Syn4$)	Mod
1	−0.554 + 6.784	1.079	0.0813	0	8.94e-04	5.95e-04	0.2258	0.2974	Local mod-
2	−0.554 − 6.784	1.079	0.0813	0	8.94e-04	5.95e-04	0.2258	0.2974	Local mod-
3	−0.689 + 7.150	1.137	0.0959	0	0.3443	0.1825	1.85e-04	7.44e-04	Local mod-
4	−0.689 − 7.150	1.137	0.0959	0	0.3443	0.1825	1.85e-04	7.44e-04	Local mod-
5	−0.058 + 3.625	0.576	0.0159	0	0.0824	0.1395	0.1605	0.1282	Interarea mod
6	−0.058 − 3.625	0.576	0.0159	0	0.0824	0.1395	0.1605	0.1282	Interarea mod

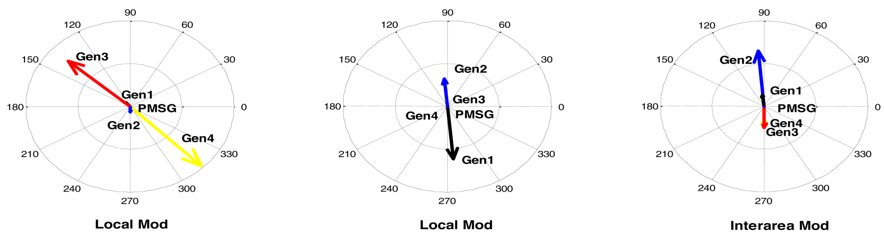

Fig. 9. Mode shapes of rotor angle modes for Kundur's two-area power system case 3.

In Fig. 12 and Table V, the results of eigenvalue analysis for IEEE 30-bus test system case 2 are given. In addition, the results of the sensitivity analysis performed for IEEE 30-bus test system case 2 are given in Table V. Finally, the mode shapes of case 2 are shown in Fig. 13.

When Fig. 12 is examined, the power system is stable because all of the eigenvalues of the power system are on the left side of the imaginary axis. In case 2, sensitivity analysis results showed that there are four local modes and one interarea mode oscillations in this power system.

In the IEEE 30-bus test system, the synchronous generator at bus 2 is replaced by PMSG-based WTG with the same power. When the effects of the PMSG-based WTG addition on the local and interarea modes of the system were investigated, it decreased the damping value of the interarea modes of the system and caused a negative effect on oscillatory stability. When the effects of the PMSG-based WTG displacement with the SG on local modes are examined, there is no effect of PMSG-based WTG displacement on local modes 1 and 4 where Gen2 is not active in case 1, as the WTG does not affect the local mode in distant areas. In case 2, for local mode 2, where Gen5 and Gen6 are active, the damping ratio of the local mode has improved as Gen3 and Gen4, attends instead of Gen2 in this mode. In case 2 for local mode 3, where Gen2, Gen3, and Gen4 are active, the damping ratio of the local mode has worsened as Gen1, which is located at a further distance to Gen3 and Gen4, attends instead of Gen2 in this mode. Oscillating concerns in the power system originate from the synchronous generator with regards to mechanical

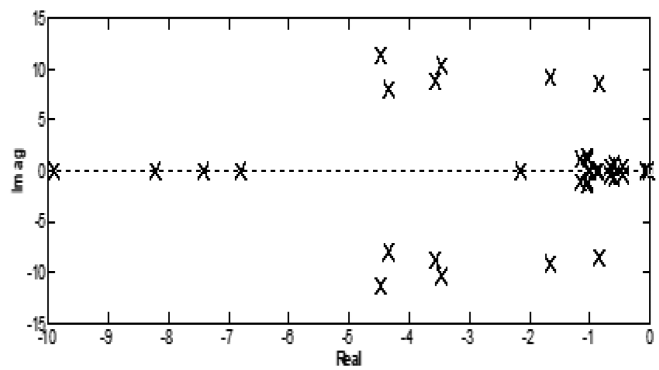

Fig. 10. Eigenvalues for IEEE 30-bus test system case 1.

TABLE IV.
EIGENVALUES AND PARTICIPATION FACTORS FOR IEEE 30-BUS TEST SYSTEM CASE 1

				Participation Factor						
EM Mod	Eigenvalue	Freq.	Damping	Gen1 (ΔSyn1 ωSyn1)	Gen2 (ΔSyn2 ωSyn2)	Gen3 (ΔSyn3 ωSyn3)	Gen4 (ΔSyn4 ωSyn4)	Gen5 (ΔSyn5 ωSyn5)	Gen6 (ΔSyn6 ωSyn6)	Mod
1	−4.473 + 11.299	1.798	0.368	2.42e-5	5.02e-4	1.86e-4	4.97e-4	0.4391	0.3498	Local mod
2	−4.473 − 11.299	1.798	0.368	2.42e-5	5.02e-4	1.86e-4	4.97e-4	0.4391	0.3498	Local mod
3	−3.467 + 10.344	1.646	0.317	9.37e-4	0.1314	0.0173	0.0448	0.3056	0.3978	Local mod
4	−3.467 − 10.344	1.646	0.317	9.37e-4	0.1314	0.0173	0.0448	0.3056	0.3978	Local mod
5	−3.567 + 8.567	1.400	0.375	0.0225	0.1846	0.5382	0.2044	0.0471	0.0645	Local mod
6	−3.567 − 8.767	1.400	0.375	0.0225	0.1846	0.5382	0.2044	0.0471	0.0645	Local mod
7	−4.346 + 8.005	1.274	0.477	0.0020	0.0074	0.2231	0.6630	0.0070	0.0104	Local mod
8	−4.346 − 8.005	1.274	0.477	0.0020	0.0074	0.2231	0.6630	0.0070	0.0104	Local mod
9	−1.038 + 1.084	0.172	0.691	0.4650	0.1370	0.0391	0.0412	0.0198	0.0197	Interarea mod
10	−1.038 − 1.084	0.172	0.691	0.4650	0.1370	0.0391	0.0412	0.0198	0.0197	Interarea mod

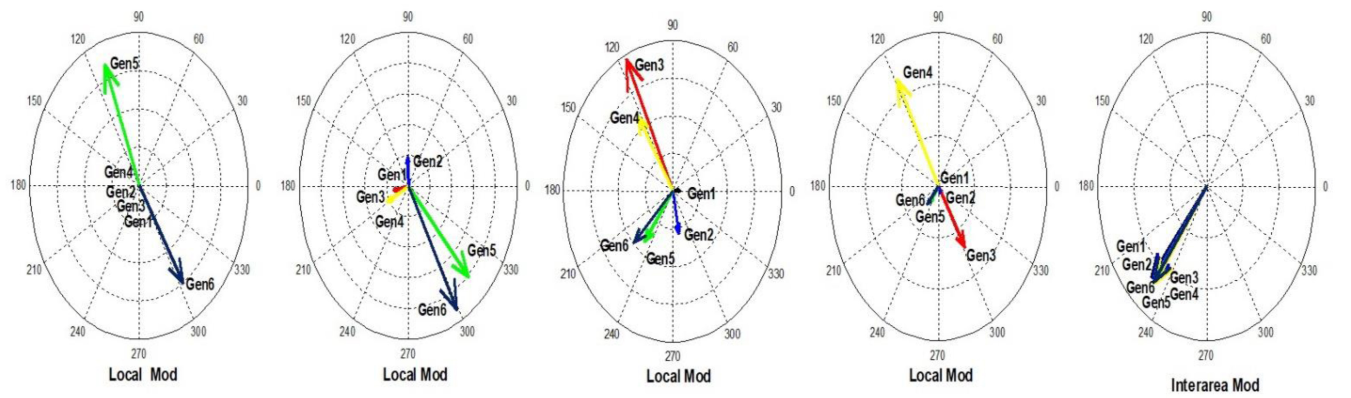

Fig. 11. Mode shapes of rotor angle modes for the IEEE 30-bus test system case 1.

speed and rotor angle swing. Due to the displacement of the generated power from the synchronous generator to the WTG, the existing electromechanical oscillations might be lost or experience path changes [46]. The experienced paths of the oscillations have changed for this situation.

Generators that contribute most to production for the IEEE 30-bus test system are Gen1 and Gen2. As can be seen in Table IV for case 1, the most important participation in the interarea mode is from Gen1 and Gen2. With the addition of the PMSG-based WTG to the system instead of Gen2, the damping rate of this mode has worsened due to the removal of the effect of Gen2 to the damping torque of the interarea mode. The undamped oscillation risk in power systems can be caused by large synchronous generator concentrations and comparatively weak links [41]. If a generator usually matches poorly with the remainder of the power system and is larger than the power system size, the damping rate in this area will decrease.

Mode shapes for case 2 are shown in Fig. 13. As can be seen from the mode figures and Table V, the mode with 0.247 Hz frequency is an interarea mode, and all generators contribute to this mode. Gen 5-6, Gen 3-4-5-6, Gen 1-3-4, and Gen 3-4 contribute to the local modes with 1.798, 1.572, 1.355, and 1,278 Hz frequency respectively.

In Fig. 14 and Table VI, the results of eigenvalue analysis for IEEE 30-bus test system case 3. are given. In addition, the results of the sensitivity analysis performed for IEEE 30-bus test system case 3 are given in Table VI. Finally, the mode shapes of case 3 are shown in Fig. 15.

When Fig. 14 is examined, the power system is stable because all of the eigenvalues of the power system are on the left side of the imaginary axis. In case 3, sensitivity analysis results showed that there are four local modes and one interarea mode oscillations in this power system.

In the IEEE 30-bus test system for case 3, a PMSG-based WTG with a power of half of Gen2 is added to bus 2 for the base case system. By adding the PMSG-based WTG to the power system, existing synchronous generators contribute less to meeting power demand. However, because the system topology remains unchanged, the ratio of synchronous generators to the impedance of the network will be reduced. Therefore, in many cases, the joint coupling will be strengthened. The strengthening of this joint coupling allows damping oscillations between synchronous generators [41]. As a result, the damping ratio of the local modes 2 and 3 with 1.633 and 1.325 Hz frequency between Gen1 and Gen2 will increase. Since WTG does not affect the local mode in distant areas, there is no effect on the local modes 1 and 4 with 1.798 and 1.262 Hz frequency.

The undamped oscillation risk in power systems can be caused by large synchronous generator concentrations and comparatively weak links [41]. If a generator usually matches poorly with the remainder of the power system and is larger than the power system size, the damping rate in this area will decrease. With the addition of PMSG-based WTG, the production of Gen2, which is one of the two main generators contributing to the production, decreases. As a result, Gen1 and Gen2 are worse matched to each other, and the contribution of Gen2 to damping torque and the rate of interarea damping decreases.

Mode shapes for case 3 are shown in Fig. 15. As can be seen from the mode figures and Table VI, the mode with 0.179 Hz frequency is an interarea mode, and all generators contribute to this mode. Gen 5-6, Gen 5-6, Gen 2-3, and Gen 3-4 contribute to the local modes with 1.798, 1.633, 1.325, and 1.262 Hz frequency. respectively.

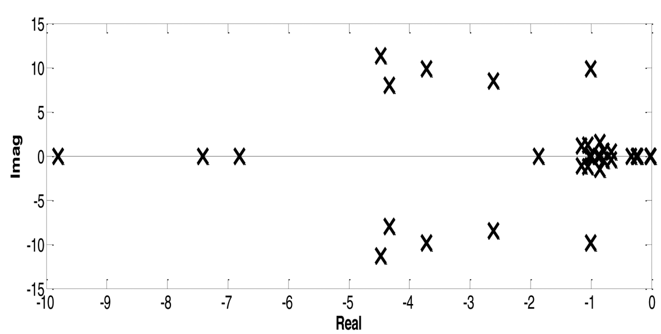

Fig. 12. Eigenvalues for IEEE 30-bus test system case 2.

TABLE V.
EIGENVALUES AND PARTICIPATION FACTORS FOR IEEE 30-BUS TEST SYSTEM CASE 2

				Participation Factor						
EM Mod	***Eigenvalue***	***Freq***	***Damping***	***Gen1 (ΔSyn1 ωSyn1)***	***DDSG ωddsg***	***Gen3 (ΔSyn3 ωSyn3)***	***Gen4 (ΔSyn4 ωSyn4)***	***Gen5 (ΔSyn5 ωSyn5)***	***Gen6 (ΔSyn6 ωSyn6)***	***Mod***
1	−4.473 + 11.299	1.798	0.368	1.02e-04	0	4.0e-04	6.54e-04	0.436	0.345	Local mod
2	−4.473 − 11.299	1.798	0.368	1.02e-04	0	4.0e-04	6.54e-04	0.436	0.345	Local mod
3	−3.721 − 9.881	1.572	0.352	0.022	0	0.145	0.139	0.297	0.415	Local mod
4	−3.721 − 9.881	1.572	0.352	0.022	0	0.145	0.139	0.297	0.415	Local mod
5	−2.615 + 8.519	1.355	0.293	0.137	0	0.345	0.241	0.074	0.094	Local mod
6	−2.615 − 8.519	1.355	0.293	0.137	0	0.345	0.241	0.074	0.094	Local mod
7	−4.330 – 8.03	1.278	0.474	0.002	0	0.297	0.591	0.0073	0.010	Local mod
8	−4.330 – 8.03	1.278	0.474	0.002	0	0.297	0.591	0.0073	0.010	Local mod
9	–0.857 + 1.552	0.247	0.483	0.406	0	0.031	0.032	0.013	0.014	Interarea mod
10	–0.857 – 1.552	0.247	0.483	0.406	0	0.031	0.032	0.013	0.014	Interarea mod

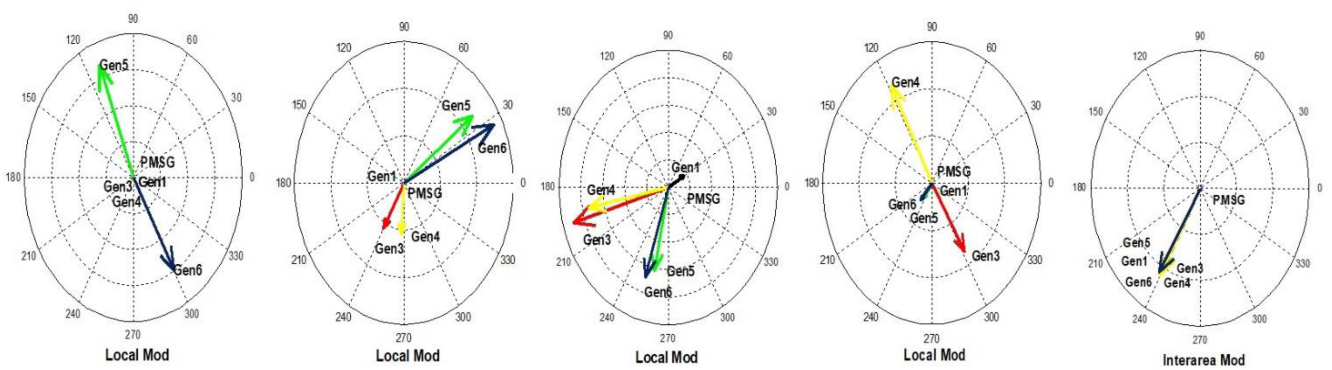

Fig. 13. Mode shapes of rotor angle modes for the IEEE 30-bus test system case 1.

V. DISCUSSION

In this study, we examine the impact of PMSG-based WTGs on power system oscillation stability, employing eigenvalue and sensitivity analysis. The analysis is conducted on two widely utilized test systems: the two-area power system proposed by Kundur and the IEEE 30-bus test system. In order to evaluate the impact of PMSG-based WTGs on both local and interarea oscillations, three different scenarios are considered. It can be concluded that the addition of a PMSG-based WTG to a power system may result in the disappearance of existing local and cross-area modes or alternatively, in path changes or a remaining constant state, depending on the location and power ratings of the PMSG-based WTG and synchronous generators in question. Upon evaluation of the results obtained from the study in general, it can be concluded that PMSG-based WTGs have the potential to exert either positive or negative effects on the damping of both local and cross-domain oscillations, depending on the specific characteristics of the WTGs and the power systems in question.

In the context of Kundur's two-field power system: In the base case (Case 1), the results of the eigenvalue analysis indicated the presence of two local modes at 1.049 Hz (field 1) and 1.08 Hz (field 2), as well as an inter-field mode at 0.53 Hz. All eigenvalues were situated to the left of the imaginary axis, indicating that the system was stable with well-damped oscillations. Upon replacing the synchronous generator with a PMSG-based WTG (Case 2), the interarea mode exhibited enhanced damping, with a corresponding increase in frequency to 0.675 Hz and 0.468 Hz. The local modes remained unaltered. The PMSG-based WTG contributed to the damping of the interarea mode due to its disconnection from the grid, thereby increasing the stability of the system oscillations. In Case 3, the introduction of a PMSG-based WTG resulted in a favorable impact on the local modes, with an enhancement in the damping of the mode between Gen1 and Gen2 (frequency at 1.113 Hz). However, the addition of the WTG resulted in a negative effect on the interarea mode with reduced damping (at frequency 0.576

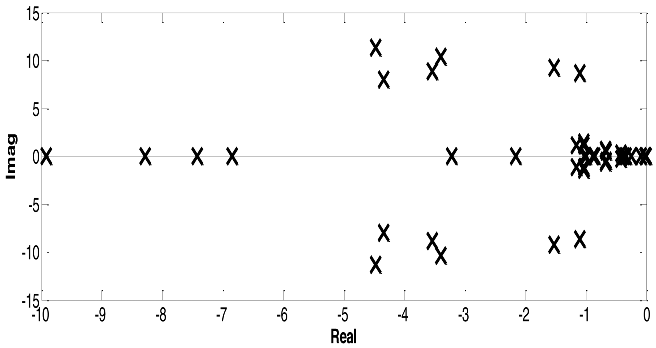

Fig. 14. Eigenvalues for IEEE 30-bus test system case 3.

Hz), potentially due to the mismatch between fields resulting from the change in production dynamics.

IEEE 30-Bus Test System: In the base case (Case 1), the system was observed to be stable with four local modes at frequencies of 1.798 Hz, 1.646 Hz, 1.4 Hz, and 1.247 Hz, and one inter-domain mode at 0.172 Hz. All eigenvalues were located to the left of the imaginary axis, indicating effective damping for both local and inter-field oscillations. In Case 2, in which a PMSG-based WTG was substituted for a synchronous generator, the damping of the inter-field mode was found to have deteriorated (frequency 0.247 Hz), primarily due to the cessation of the contribution of Gen2 to the damping torque. However, the damping of local modes with Gen5 and Gen6 active showed an improvement, which serves to illustrate that PMSG-based

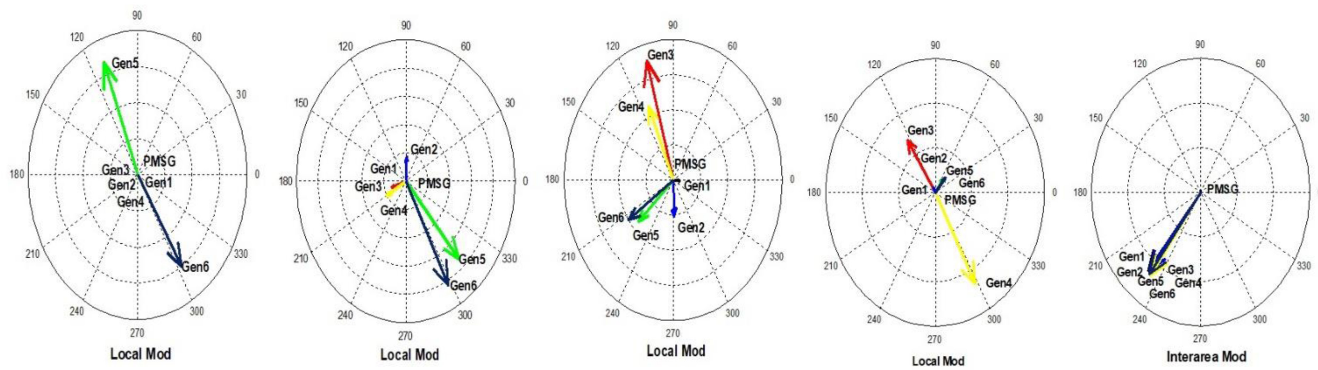

Fig. 15. Mode shapes of rotor angle modes for the IEEE 30-bus test system case 3.

TABLE VI.
EIGENVALUES AND PARTICIPATION FACTORS FOR IEEE 30-BUS TEST SYSTEM CASE 3

EM Mod	*Eigenvalue*	*Freq*	*Damping*	*Participation Factor* *Gen1 (ΔSyn1 ωSyn1)*	*DDSG ωDdsg*	*Gen2 (ΔSyn2 ωSyn2)*	*Gen3 (ΔSyn3 ωSyn3)*	*Gen4 (ΔSyn4 ωSyn4)*	*Gen5 (ΔSyn5 ωSyn5)*	*Gen6 (ΔSyn6 ωSyn6)*	*Mod*
1	–4.437 + 11.298	1.798	0.365	2.8e-04	0	4.6e-04	1.8e-04	4.9e-04	0.437	0.351	Local mod
2	–43437 – 11.298	1.798	0.365	2.8e-04	0	4.6e-04	1.8e-04	4.9e-04	0.437	0.351	Local mod
3	–3.401 + 10.344	1.644	0.312	0.001	0	0.142	0.022	0.051	0.314	0.404	Local mod
4	–3.401 – 10.344	1.644	0.312	0.001	0	0.142	0.022	0.051	0.314	0.404	Local mod
5	–1.105 – 8.668	1.379	0.126	0.169	0	0.251	0.046	0.037	0.019	0.022	Local mod
6	–1.105 – 8.668	1.379	0.126	0.169	0	0.251	0.046	0.037	0.019	0.022	Local mod
7	–3.535 + 8.861	1.410	0.370	0.025	0	0.182	0.542	0.226	0.060	0.081	Local mod
8	–3.535 – 8.861	1.410	0.370	0.025	0	0.182	0.542	0.226	0.060	0.081	Local mod
9	–4.343 + 8.013	1.275	0.476	0.002	0	0.006	0.230	0.656	0.007	0.010	Local mod
10	–4.343 – 8.013	1.275	0.476	0.002	0	0.006	0.230	0.656	0.007	0.010	Local mod
11	–1.033 + 1.124	0.178	0.676	0.456	0	0.134	0.038	0.040	0.019	0.019	Interarea mod
12	–1.033 – 1.124	0.178	0.676	0.456	0	0.134	0.038	0.040	0.019	0.019	Interarea mod

WTGs exert different effects on different oscillation modes. In Case 3, where a PMSG-based WTG was introduced, the damping of the local modes was found to have improved further, particularly for the mode situated between Gen1 and Gen2, where the frequency was 1.633 Hz. However, the interarea mode continued to demonstrate reduced damping (frequency 0.179 Hz), reflecting the challenges associated with the large-scale integration of PMSG-based WTGs in maintaining stability across all oscillation modes.

V. CONCLUSION

This paper's focus on PMSG-based WTGs, its detailed oscillatory stability analysis, its comparative case study approach, and its modern relevance to renewable energy challenges represent its main innovations, distinguishing it from existing literature. The following section itemizes these innovations.

- While numerous preceding studies have concentrated on the stability analysis of DFIGs, this paper is among a limited number that have specifically investigated the effects of PMSGs on local and in-field oscillations through the use of eigenvalue and sensitivity analysis. This constitutes a significant contribution to the field, given that the majority of existing literature pertains to alternative WTG types. The distinctive features of the PMSG, including its separation from the grid through the use of power electronics, provide novel insights into system dynamics.
- This study highlights the paucity of research on the impact of PMSG-based WTGs on oscillatory modes in power systems, despite extensive studies on the effects of DFIG-based WTGs on oscillatory modes in terms of mode shapes and sensitivity analysis. This study addresses this gap by providing a comprehensive analysis of the role of PMSGs in power system oscillations and offering new insights into both the methodology and the findings of previous studies.
- This study presents a three-scenario comparison (base case, replacement of synchronous generators with PMSG-based WTGs, and addition of PMSG-based WTGs on different busbars) that provides a comprehensive understanding of the impact of the placement and capacity of PMSG-based WTGs on power system stability.
- While there is a substantial body of literature on the use of eigenvalue analysis in stability studies, the application of this method to Kundur's two-area system and the IEEE 30-bus test system, with a particular focus on PMSG-based WTGs, offers a novel perspective on the behavior of these systems in the context of modern wind generation technology.
- This study examines the influence of PMSG-based WTG placement and power ratings on oscillatory stability. The impact of WTG location and generator power on both local and in-field oscillations is analyzed in detail.
- A principal finding of this study is that PMSG-based WTGs can diminish or have a negligible effect on local modes due to their separation from the power grid via power electronics. However, they can significantly affect in-field modes. It demonstrates that PMSG-based WTGs do not react to system oscillations in the same manner as synchronous generators or other types of WTGs, resulting in a distinct dynamic response.

Availability of Data and Materials: The data that support the findings of this study are available on request from the corresponding author.

Peer-review: Externally peer-reviewed.

Author Contributions: Concept – C.H., B.Y.; Design – C.H., B.Y.,;Supervision – C.H., B.Y., H.K., M.T.Ö.; Resources – C.H., B.Y.; Materials – C.H., B.Y.; Data Collection and/or Processing – C.H., B.Y.; Analysis and/or Interpretation –C.H., B.Y., H.K., M.T.Ö.; Literature Search – C.H., B.Y., H.K., M.T.Ö.; Writing – C.H., B.Y., H.K., M.T.Ö.; Critical Review – C.H., B.Y., H.K., M.T.Ö.

Declaration of Interests: The authors have no conflicts of interest to declare.

Funding: This study received no funding.

REFERENCES

1. B. Yildirim, Eigenvalue Sensitivity and Oscillatory Stability Analysis of Wind Turbine System with Squirrel Cage Induction Generator, Science and Eng. J of Firat University, Vol. 30, pp. 239–247, 2018
2. A. Ahmadi et al., "Recent residential applications of low-temperature solar collector," *J. Cleaner Prod.*, vol. 279, 2021. [CrossRef]
3. H. Acaroğlu, and M. Güllü, "Climate change caused by renewable and non-renewable energy consumption and economic growth: A time series ARDL analysis for Turkey," *Renew. Energy*, vol. 193, 434–447, May 2022. [CrossRef]
4. A. Kocalmis Bilhan, "Integrated solar-based PEMWEs for green electricity production," *Int. J. Hydrog. Energy*, vol. 75, pp. 415–427, 2024. [CrossRef]
5. G. Bayrak, A. Küçüker, and A. Yılmaz, "Deep learning-based multi-model ensemble method for classification of PQDs in a hydrogen energy-based microgrid using modified weighted majority algorithm," *Int. J. Hydrog. Energy*, vol. 48, no. 18, pp. 6824–6836, 2023. [CrossRef]
6. R. Çakmak, H. Meral, and G. Bayrak, "A new intelligent charging strategy in a stationary hydrogen energy-based power plant for optimal demand side management of plug-in EVs," *Int. J. Hydrog. Energy*, vol. 75, 400–414, 2024. [CrossRef]
7. C. Haydaroğlu, H. Kılıç, and B. Gümüş, "Performance analysis and comparison of performance ratio of solar power plant," *Turk. J. Electr. Power Energy Syst.*, vol. 4, No. 3, 190–199, Sep. 2024. [CrossRef]
8. International Energy Agency, "International Energy Agency (IEA) world energy outlook 2022,"2022, p. 524. Available: https://Www.Iea.Org/Reports/World-Energy-Outlook-2022/Executive-Summary.
9. IEA, Electricity Market 2023, 2023. Available: https://www.iea.org/reports/electricity-market-report-2023.
10. *Global Wind Report 2024*. Available: https://gwec.net/global-wind-report-2024/.
11. "Global-offshore-wind-report2024". Available: https://gwec.net/global-offshore-wind-report-2024/.
12. B. Yildirim, and M. T. Ozdemir, "An overview of the power of wind energy in the world, EJONS International Journal on Mathematic, Engineering and Natural Sciences," vol. 2, no. 1, pp. 33–39, 2018.
13. I. C. Gil-García, A. Ramos-Escudero, M. S. García-Cascales, H. Dagher, and A. Molina-García, "Fuzzy GIS-based MCDM solution for the optimal offshore wind site selection: The Gulf of Maine case," *Renew. Energy*, vol. 183, pp. 130–147, Jan. 2022. [CrossRef]
14. A. A. B. Mohd Zin, M. Pesaran, A. B. Khairuddin, L. Jahanshaloo, and O. Shariati, "An overview on doubly fed induction generators controls and contributions to wind based electricity generation," *Renew. Sustain. Energy Rev.*, vol. 27, pp. 692–708, 2013. [CrossRef]
15. S. H. Qazi, and M. W. Mustafa, "Review on active filters and its performance with grid connected fixed and variable speed wind turbine generator," *Renew. Sustain. Energy Rev.*, vol. 57, pp. 420–438, 2016. [CrossRef]

16. Z. Wu, X. Dou, J. Chu, and M. Hu, "Operation and control of a direct-driven PMSG-based wind turbine system with an auxiliary parallel grid-side converter," *Energies*, vol. 6, no. 7, pp. 3405–3421, 2013. [CrossRef]
17. A. Bonfiglio, F. Delfino, F. Gonzalez-Longatt, and R. Procopio, "Steady-state assessments of PMSGs in wind generating units," *Int. J. Electr. Power Energy Syst.*, vol. 90, pp. 87–93, 2017. [CrossRef]
18. N. P. W. Strachan, and D. Jovcic, "Dynamic modelling, simulation and analysis of an offshore variable-speed directly-driven permanent-magnet Wind Energy Conversion and Storage System (WECSS)," OCEANS 2007, 18–21 June, 2007. [CrossRef]
19. F. Xiao, Y. Xia, K. Zhang, H. Li, K. Chen, and P. Li, "Study on a small-signal analysis method for PMSG considering LVRT control and frequency regulation," *IET Gener. Transm. Distrib.*, vol. 16, no. 11, pp. 2154–2165, Jun. 2022. [CrossRef]
20. L. P. Kunjumuhammed, B. C. Pal, R. Gupta, and K. J. Dyke, "Stability analysis of a PMSG-based large offshore wind farm connected to a VSC-HVDC," *IEEE Trans. Energy Convers.*, vol. 32, no. 3, pp. 1166–1176, 2017. [CrossRef]
21. H. Ye, Y. Tang, W. Pei, and L. Kong, "Numerical stability analysis of PMSG-based wind energy conversion system: A simple example of drive system," *J. Eng.*, vol. 2017, no. 13, pp. 955–960, 2017. [CrossRef]
22. M. Rahimi, "Modeling, control and stability analysis of grid connected PMSG based wind turbine assisted with diode rectifier and boost converter," *Int. J. Electr. Power Energy Syst.*, vol. 93, pp. 84–96, 2017. [CrossRef]
23. M. Chouket, and L. Krichen, Small Signal Modeling and Stability Analysis of Wind Turbine with PMSG Connected to the Grid, IEEE 12th International Multi- Conference on Systems, Signals & Devices (SSD 2015), 16–19 March, 2015.
24. S. Y. Kong, R. C. Bansal, and Z. Y. Dong, "Comparative small-signal stability analyses of PMSG-, DFIG- and SCIG based wind farms," *Int. J. Ambient Energy*, vol. 33, no. 2, pp. 87–97, 2012. [CrossRef]
25. D. R. Chandra et al, "Impact of SCIG, DFIG wind power plant on IEEE 14 bus system with small signal stability assessment", 18th National Power Systems Conference (NPSC), 18–20 Dec., 2014. [CrossRef]
26. P. He, F. Wen, G. Ledwich, Y. Xue, and J. Huang, "Investigation of the effects of various types of wind turbine generators on power-system stability," *J. Energy Eng.*, vol. 141, no. 3, pp. 1–10, 2015. [CrossRef]
27. P. He, F. Wen, G. Ledwich, and Y. Xue, "An investigation on interarea mode oscillations of interconnected power systems with integrated wind farms," *Int. J. Electr. Power Energy Syst.*, vol. 78, pp. 148–157, 2016. [CrossRef]
28. N. R. Chaudhuri, and B. Chaudhuri, "Considerations toward coordinated control of DFIG-based wind farms," *IEEE Trans. Power Deliv.*, vol. 28, no. 3, pp. 1263–1270, 2013. [CrossRef]
29. Y. Yang, Y. Li, X. Yuan, J. Li, and Z. Du, "Damping torque analysis of the PMSG-based WT with supplementary damping control for mitigating interarea oscillations," *Int. Trans. Electr. Energy Syst.*, vol. 2022, pp. 1–15, Nov. 2022. [CrossRef]
30. L. Sun, and X. Zhao, "Modelling and analysis of frequency-responsive wind turbine involved in power system ultra-low frequency oscillation," *IEEE Trans. Sustain. Energy*, vol. 13, no. 2, pp. 844–855, Apr. 2022. [CrossRef]
31. L. Wang et al., "Dominant inter-area oscillation mode identification using local measurement and modal energy for large-scale power systems with high grid-tied VSCs penetration," *Int. J. Electr. Power Energy Syst.*, vol. 117, no. October, p. 105697, 2020. [CrossRef]
32. C. Liu, S. Yu, Y. Zhang, S. Diao, and X. Zhao, "Dominant inter-area oscillation path analysis of power systems with a high penetration of permanent magnet synchronous generator by using network mode energy," *IET Gener. Transm. Distrib.*, vol. 15, no. 23, pp. 3326–3344, Dec. 2021. [CrossRef]
33. O. M. Kamel, A. Y. Abdelaziz, and A. A. Z. Diab, "Damping oscillation techniques for wind farm DFIG integrated into inter-connected power system," *Electr. Power Compon. Syst.*, vol. 48, no. 14–15, pp. 1551–1570, 2020. [CrossRef]
34. M. Basu, J. Kim, R. M. Nelms, and E. Muljadi, "Interarea-oscillation damping with dual power oscillation damping controller of a utility-scale wind power plant," 2021 3rd International Conference on High Voltage Engineering and Power Systems, ICHVEPS 2021, pp. 581–585, 2021. [CrossRef]
35. P. Kundur et al, "Definition and classification of power system stability IEEE/CIGRE joint task force on stability terms and definitions," *IEEE Trans. Power Syst.*, vol. 19, no. 3, pp. 1387–1401, 2004. [CrossRef]
36. D. Mondal, A. Chakrabarti, and A. Sengupta, *Power System Small Signal Stability Analysis and Control*. Amsterdam: Elsevier, 2014.
37. A. Gomez-Exposito, A. J. Coneho, and C. Canizares, *Electric Energy Systems Analysis and Operation*. CRC Pres Taylor@Francis Group, 2009.
38. P. W. Sauer, and M. A. Pai, *Power System Dynamics and Stability*. Singapore: Pearson Education Pte. Ltd., 1998.
39. B. Yildirim, and M. T. Gencoglu, "Oscillatory stability and eigenvalue analysis of power system with microgrid," *Electr. Eng.*, vol. 100, no. 4, pp. 2351–2360, 2018. [CrossRef]
40. A. U. Krismanto, N. Mithulananthan, and I. Kamwa, "Oscillatory stability assessment of microgrid in autonomous operation with uncertainties," *IET Renew. Power Gener.*, vol. 12, no. 4, pp. 494–504, 2018. [CrossRef]
41. P. Kundur, *Power System Stability and Control*. New York: McGraw-hill, 1994.
42. F. Milano, *Power System Modelling and Scripting*. New York: Springer London Dordrecht Heidelberg, 2010.
43. "Power systems test case archive". Available: https://www2.ee.washington.edu/research/pstca/pf30/pg tca30bus.htm.
44. J. L. Rueda, and I. Erlich, "Impacts of large scale integration of wind power on power system small-signal stability". 4. International Conference on Electric Utility Deregulation and Restructuring and Power Technologies (DRPT), 6–9 July, 2011. [CrossRef]
45. T. Ackermann, *Wind Power in Power Systems*. Wiley Online Library, 2005.
46. A. U. Krismanto, M. Nadarajah, and O. Krause, "Inuence of renewable energy based microgrid on low frequency oscillation of power systems" 2015 IEEE PES Asia-Pacific Power and Energy Engineering Conference (APPEEC), 15-18 Nov, 2015.